Local SARS-CoV-2 peptide-specific Immune Responses in Convalescent and Uninfected Human Lung Tissue Models

Kayla F. Goliwas[1], Christopher S. Simmons[1], Saad A. Khan[1], Anthony M. Wood[1], Yong Wang[1], Joel L. Berry[2], Mohammad Athar[3], James A. Mobley[4], Young-il Kim[5], Victor J. Thannickal[6], Kevin S. Harrod[4], James M. Donahue[7] and Jessy S. Deshane[1*].

[1] Department of Medicine
Division of Pulmonary, Allergy, and Critical Care Medicine
University of Alabama at Birmingham
Birmingham, AL

[2] Department of Biomedical Engineering
University of Alabama at Birmingham
Birmingham, AL

[3] Department of Dermatology
University of Alabama at Birmingham
Birmingham, AL

[4] Department of Anesthesiology and Perioperative Medicine
University of Alabama at Birmingham
Birmingham, AL

[5] Department of Medicine, Division of Preventative Medicine
University of Alabama at Birmingham
Birmingham, AL

[6] Department of Medicine,
Tulane University School of Medicine

[7] Department of Surgery
University of Alabama at Birmingham
Birmingham, AL

* Corresponding author:
Jessy S. Deshane
Associate Professor
Department of Medicine
Division of Pulmonary Allergy and Critical Care Medicine
THT 433A, 1900 University Boulevard
University of Alabama at Birmingham
Birmingham, AL 35294-0006
(205) 996-2041
jessydeshane@uabmc.edu

SUMMARY

Multi-specific and long-lasting T cell immunity have been recognized as indicators for long term protection against pathogens including the novel coronavirus SARS-CoV-2, the causative agent of the COVID-19 pandemic. Functional significance of peripheral memory T cell subsets in COVID-19 convalescents (CONV) are beginning to be appreciated; but little is known about lung resident memory T cell (lung TRM) responses and their role in limiting the severity of SARS-CoV-2 infection. Here, we utilize a perfusion three dimensional (3D) human lung tissue model and identify pre-existing local T cell immunity against SARS-CoV-2 spike protein and structural antigens in the lung tissues. We report *ex vivo* maintenance of functional multi-specific IFN-γ secreting lung TRM in CONV and their induction in lung tissues of vaccinated CONV. Importantly, we identify SARS-CoV-2 spike peptide-responding B cells in lung tissues of CONV in *ex vivo* 3D-tissue models. Our study highlights a balanced and local anti-viral immune response in the lung and persistent induction of TRM cells as an essential component for future protection against SARS-CoV-2 infection. Further, our data suggest that inclusion of multiple viral antigens in vaccine approaches may broaden the functional profile of memory T cells to combat the severity of coronavirus infection.

INTRODUCTION

COVID-19, the disease caused by the novel coronavirus SARS-CoV-2, has been a global health concern worldwide for the past two years[1-3]. This pandemic has claimed millions of lives and has caused significant economic impacts[1-3]. Infected individuals develop lymphopenia and demonstrate hyperactivated and exhausted T cell responses that contribute to the prolonged period of immune dysregulation, an established hallmark of SARS-CoV-2 infection[4-8]. Although vaccine efforts have been successful, the emergence of variants[9, 10], persistence of infection rates and lack of adequate vaccine intake continue to pose a problem for eradication and management of COVID-19. All current COVID-19 vaccines utilize SARS-CoV-2 spike protein to elicit humoral immunity. However, whether these approaches will induce long-term protection is largely unknown.

Evidence from previous zoonotic coronaviruses indicate that an important determinant for recovery and long-term protection is coronavirus-specific T cell immunity[11-13]. During the initial phase of the pandemic, 20-50% unexposed individuals had significant T cell reactivity to SARS-CoV-2 antigen peptide pools[6, 7, 14-17]. Several studies reported pre-existing CD4 and CD8 T cell responses in peripheral blood mononuclear cells against both structural (nucleocapsid, N) and non-structural regions of SARS-CoV-2 in COVID-19 convalescent individuals[6, 7, 14-23]. In majority of the convalescents (CONV), SARS-CoV-2-specific CD4 and CD8 T cell responses are seen with significantly larger overall T cell responses in those who had severe compared with mild disease[18, 22, 23]. However, a greater proportion of $CD8^+$ compared with $CD4^+$ T cell responses were noted in mild cases[18, 22, 23]. Additionally, polyfunctional $CD8^+$ T cells were increased in mild versus severe disease. Furthermore, long-lasting memory T cells reactive to N protein of SARS-CoV, displayed robust cross-reactivity to N protein of SARS-CoV-2[24, 25]. Interestingly, SARS-CoV-2-specfic T cells are present in individuals with no prior history of SARS suggesting the possibility of pre-existing cross-reactive immune memory to seasonal coronaviruses[7, 17].

As memory T cell response induced by previous viral pathogens can shape susceptibility to subsequent viral infections including SARS-CoV-2, and/or influence clinical severity of COVID-19, pre-existing memory T cells that recognize SARS-CoV-2 have been evaluated recently[22, 24-29]. Upon SARS-CoV-2 exposure, individuals with pre-existing T cell immunity are anticipated to have a faster and stronger immune response that could limit disease severity[7]. Additionally, increased memory T follicular helper $CD4^+$ T cells could facilitate a rapid SARS-CoV-2 neutralizing antibody response[30]. The increased presence of both memory $CD4^+$ and $CD8^+$ T cells may enable direct antiviral immunity in the lungs and nasopharynx; pre-existing $CD4^+$ T cell memory could influence the outcome of vaccination, leading to a quicker robust immune response and development of neutralizing antibodies[31]. Alternatively, pre-existing immunity could be detrimental due to antibody-mediated disease enhancement or from an inferior immune response[32]. Thus accurate measurements of pre-existing T cell immunity are essential to correlate with prospective infection, disease severity and effective vaccine responses.

The assessment of a complete SARS-CoV-2 reactive T cell pool in circulation of uninfected (UN) and CONV individuals has been challenging. A full understanding of both the breadth and depth of the SARS-CoV-2 specific T cell responses have not been accomplished so far, as studies have been restricted to circulating T cells which may not adequately represent lung-specific responses to viral infection and/or may not reflect direct anti-viral immunity in the lungs or the nasopharynx. We have developed a perfused three dimensional lung tissue culture model that maintains the tissue architecture of the human lung and enables assessment of pre-existing T cell immunity in the lung tissue. Utilizing this model established with lung tissue cores from both UN and CONV individuals, we demonstrate the presence of local immune responses to SARS-CoV-2 peptide pools in the lungs of UN individuals induced by pre-existing T cell immunity and significant memory T cell response in the lungs of CONV individuals.

RESULTS

Ex Vivo Perfusion Culture of Human Lung Tissues

We first collected remnant surgical specimen from individuals without any history of SARS-CoV-2 infection, who were undergoing lung resection surgeries. For *ex vivo* culture, 5 mm diameter tissue cores were generated and one tissue core was placed into the central chamber of a polydimethylsiloxane (PDMS) bioreactor containing a mixture of extracellular matrix (ECM) components for structural support. The tissue/ECM support was penetrated with five 400 micron Teflon coated stainless steel wires to generate through-channels for adequate tissue perfusion. Wires were removed following ECM polymerization. The bioreactor was then connected to a perfusion system and peristaltic pump, where a serum-free defined tissue culture media was perfused from a media reservoir through the tissue volume and collected in a collection reservoir (**Figure 1A-B**). Using this culture system, we have observed maintenance of histologic tissue architecture (**Extended Fig. 1A**), as well as cell density (cells/area, **Extended Fig. 1B**) over a two week culture period. Further, lactate dehydrogenase (LDH) remained unchanged during culture (**Extended Fig. 1C**), indicating sustained viability. The ECM composition utilized in this model has been used with earlier prototype bioreactors to generate cell culture models of lung and breast carcinoma (Goliwas et. al. 2021; Goliwas et al, 2016), where cell growth and sustained viability have been observed. These platforms were adapted for the ex vivo culture of human lung tissue for these studies and cell phenotyping showed maintenance of lung epithelial and endothelial cells, as well as fibroblasts, lymphocytes including $CD8^+$ T cells (**Extended Figs. 1D-H**) and proteomics showed maintenance of the lung ECM (**Extended Fig. 1I**).

Cellular Landscape and Response to SARS-CoV-2 Peptides within the Lung Tissues of Previously Uninfected and Convalescent Individuals

Local immune response to SARS-CoV-2 peptides was compared in lung tissue specimen collected from eight individuals who were not previously infected with SARS-CoV-2 (uninfected,

UN) and four individuals who previously tested positive for SARS-CoV-2 and cleared the virus (convalescent (CONV), **Extended Data Table 1** with subject demographics). Tissue cores were cultured *ex vivo* using the bioreactor platform and following four to five days perfusion culture, peptide pools covering the SARS-CoV-2 membrane glycoprotein (M peptide), nucleocapsid phosphoprotein (N peptide), or the immunodominant sequence of the spike protein (S peptide) were added and cellular response was compared to vehicle control exposed tissues (**Figure 1C**).

While baseline cell phenotyping showed no difference in epithelial cell populations, endothelial cells, $CD45^+$ immune cells, TNF-α producing immune cells, or $CD4^+$ T cells within the lung tissues of CONV and UN individuals (**Extended Figs. 2A-C, Extended Figs. 3A-B, Extended Fig. 4A, Figure 2A-B**), a significant increase in the frequency of PD-1^+ $CD4^+$ T cells was noted (**Figure 2C**). Other subpopulations of $CD4^+$ T cells showed no difference at baseline within the lungs of CONV and UN individuals (**Figure 2D, Extended Figs. 5A-E**). The frequency of $CD8^+$ T cells was moderately increased in CONV lung tissues when compared to UN tissues (**Figure 2E**). Similar to the $CD4^+$ T cells, the PD-1^+ $CD8^+$ T cells were elevated in CONV at baseline (**Figure 2F**), but no differences were observed in other subpopulations of $CD8^+$ T cells (**Figure 2G, Extended Figs. 6A-E**). The maintenance of cell populations over the culture period was assessed, comparing UN or CONV tissues in culture to the respective starting tissues. While overall $CD45^+$ frequencies reduced over the culture period, this change in frequencies of epithelial, endothelial, T or B cell populations comparing UN and CONV tissues were not significantly different (**Extended Figs. 2D, 3C, 4B, 7, 8L-Y, & 9C-I**); naïve $CD8^+$ T cells showed a trending difference (p=0.068) following *ex vivo* culture (**Extended Fig 8S**).

Following exposure to the three peptide pools developed against structural proteins of SARS-CoV-2, the lung tissue cores were collagenase digested and alterations in the cellular landscape and immune response were evaluated. As noted at baseline, no differences were observed in the epithelial cell populations, but an increase in $CD31^+$ endothelial cells was found

with M peptide treatment in CONV samples (**Extended Fig. 2E** & **Extended Fig. 3D**). No changes were noted in the $CD45^+$ immune cells, TNF-α producing immune cells, or the $CD4^+$ T cells with peptide exposure within UN or CONV lung tissues (**Figures 2H-I, Extended Fig. 4C**). The change in frequency of the PD-1^+ $CD4^+$ T cells between control and N peptide-exposed tissues was greater in CONV compared to UN lung tissues (**Figure 2J**). Additionally, the hyperactivated $CD4^+$ T cells showed an increasing trend in CONV tissues (p=0.075) exposed to the M peptide when compared to control; this change was not observed in UN tissues (**Figure 2K**). No significant changes were noted in proliferating, antigen specific, or IFN-γ producing $CD4^+$ T cells (**Extended Figs. 5F-I**). When $CD8^+$ T cells were evaluated, the frequency of M-peptide responders showed an increasing trend (p=0.064) in the UN tissues. The change between control and N-peptide responders was significantly different between UN and CONV, with increased $CD8^+$ T cell response in CONV (**Figure 2L**). The frequency of proliferating and antigen specific $CD8^+$ T cells, although not significant (p=0.051 with M peptide exposure and p=0.093 with S peptide exposure, respectively), increased with peptide exposure in UN, but not CONV tissues (**Extended Figs. 6F-G**). No significant difference was observed in PD-1^+, hyperactivated, or IFN-γ producing $CD8^+$ T cells (**Figures 2M-N, Extended Figs. 6H-I**).

Memory T cell Response to SARS-CoV-2 Peptides within the Lung Tissues of Convalescent Individuals

We assessed T cell memory subsets within the lung tissues of UN and CONV individuals, as they play a vital role in viral clearance during re-infection and recent studies identified functional memory T cells within the peripheral blood of CONV patients[22, 24-29]. At baseline, $CD4^+$ or $CD8^+$ lung memory T cell subsets were not significantly different comparing UN and CONV tissues (**Figure 3A-J**, **Extended Figs. 8A-G**). However, tissue resident memory (TRM) and effector memory (EM) were the most prevalent subsets within the lung tissue (**Figures 3A, 3F, 3E & 3J)**. Following *ex vivo* culture, TRM responses to all peptide pools were noted within the UN tissues,

with decreasing CD4$^+$ TRM frequency with peptide exposure (**Figure 3K**). We determined the % IFN-γ^+ subsets within the CD4$^+$ and CD8$^+$ TRM as well as % TRM within the overall IFN-γ^+ CD4$^+$ and CD8$^+$ cells. Although statistical significance was not observed when comparing UN and CONV, patient-specific differences were noted in CONV. At baseline, the average % IFN-γ^+ CD8$^+$TRM in CONV was 1.71 fold higher than UN average (**Figure 3G).** Within the CONV, % IFN-γ^+ CD8$^+$TRM and % IFN-γ^+ CD4$^+$TRM in Subject #10 who received COVID-19 vaccination, were 3.69 and 4.65 fold higher, respectively, than average of UN (**Figure 3Q, 3L).** While meaningful fold change in average %TRM within CD8$^+$IFN-γ^+ was not noted, the average %TRM within CD4$^+$IFN-γ^+ in CONV was 2 fold higher than UN average (**Figure 3M).** Of the total IFN-γ^+ CD8$^+$ T cells in the lungs of CONV individuals #11 (COVID$^+$ twice) and #8, 40-50% were TRM (**Figure 3R**). Both % IFN-γ^+ of the CD8$^+$TRM (2.55 fold) and % TRM within CD4$^+$IFN-γ^+ (2.26 fold) were higher in Subject #11 (**Figure 3R, 3L**). In CONV Subject #10, S-peptide responding % IFN-γ^+ CD8$^+$TRM was 1.5 fold higher compared to control (**Figure 3Q**), and the %TRM within CD8$^+$IFN-γ^+ cells was 3.25 fold and 2.72 fold higher in M-peptide and N-peptide exposed tissues, respectively (**Figure 3R**). Interestingly, in CONV #5, % IFN-γ^+ CD8$^+$TRM was 5.88 fold and 10 fold higher in the S-peptide and M-peptide treated samples compared to the respective controls; robust response was not noted with N-peptide (**Figure 3Q**). The % TRM CD4$^+$IFN-γ^+ S-peptide responders in CONV #5 was 12.5 fold higher than the control, whereas other CONV did not demonstrate a robust response in (**Figure 3M**); in CONV #8, the M-peptide responders were 3.39 fold higher compared to control (**Figure 3M**). The % IFN-γ^+ within the CD4$^+$TRM cells that are S-peptide responders were 14.3 fold higher compared to controls in CONV #5, while the responders were minimal in CONV #10 and 11 (**Figure 3L**). But the % IFN-γ producing M-peptide responder CD4$^+$TRM were 2.87 fold and N-peptide responder TRM were 3.31 fold higher in vaccinated CONV #10 and CONV #11 (COVID$^+$ twice) respectively compared to control (**Figure 3L**).

Additionally, stem cell like $CD4^+$ memory T cells increased in frequency (p=0.078) with M peptide exposure (**Extended Fig. 8H**), whereas both naïve and central memory $CD4^+$ T cell frequencies reduced with M-peptide exposure; similar reduction in N-peptide responders within naïve $CD4^+$ T cells was noted in UN tissues (**Figures 3N, Extended Fig. 8I**). Interestingly, the change in the frequency of naïve $CD4^+$ T cells, when comparing the control and S peptide responders, was significantly increased in CONV when compared to UN (**Figure 3N**). No significant differences were observed in $CD4^+$ EM cells (**Figure 3O**). Amongst $CD8^+$ memory subsets, a trend towards a reduction in S peptide- responding TRM $CD8^+$ T cells was noted (p=0.076), when compared to respective controls in UN tissues. This trend coincided with an increasing trend in the change in frequency of TRM between control and S peptide exposure when comparing UN and CONV; this cell population increased with peptide stimulation in CONV tissues (**Figure 3P**). No differences were observed in $CD8^+$ stem cell like memory T cells and minimal changes were observed in $CD8^+$ naïve and central memory subsets (**Extended Fig. 8J-K, Figure 3S**). Importantly, $CD8^+$ effector memory cells tended to increase with peptide exposure in CONV tissues, with a significant increase in the change between control and S peptide treated samples observed in CONV tissues when compared to UN tissues (**Figure 3T**).

As the humoral immune response to infection is essential for protection and has not been evaluated in SARS-CoV-2 convalescence at the tissue level, we evaluated B cell subsets in a subset of the lung tissues from UN and CONV individuals. No significant differences in B cell subsets were noted at baseline (**Figure 4A-G, Extended Figs. 9A-B**). When $CD19^+$ B cells were evaluated following *ex vivo* culture and peptide exposure, a trend towards an increase (p=0.068) was observed in CONV tissues with S peptide exposure when compared to control. Furthermore, the change between control and S peptide exposed samples was significantly different in CONV when compared to UN tissues (**Figure 4H**). When evaluating memory B cells, opposing changes between control and M peptide exposed samples were noted in UN and CONV (**Figure 4I**). While

transitional B cells were boosted in UN, plasmablasts tended to be higher in CONV samples, and all other B cell subsets remained unchanged with peptide exposure (**Figures 4J-N**).

CONCLUSIONS

Towards optimal assessment of the impact of specific T cell and humoral responses on host protection, T cell dynamics both during SARS-CoV-2 infection and memory phase should be addressed; it is essential to evaluate the role of SARS-CoV-2 specific effector T cells for viral clearance and potential accumulation of these in CONV and recovered individuals over time. But modeling local immune responses against SARS-CoV-2 has so far posed challenges for lack of appropriate small animal models of infection and access to lung tissues from infected and convalescent individuals during this pandemic. We demonstrate here the establishment of a three dimensional perfused human lung tissue model that maintains the cellular heterogeneity, viability and human matrix components over an extended culture period. In this model, we successfully evaluate local immune response to SARS-CoV-2 peptide pools that represent membrane, nucleocapsid and spike proteins of SARS-CoV-2. We provide evidence for pre-existing T cell immunity and SARS-CoV-2 peptide-specific local lymphocyte memory responses in lung tissues from UN and CONV that validates this model for evaluating local immune responses to viral anew and previously encountered viral antigens.

Evidence of elevated frequencies of PD-1$^+$ CD4$^+$ and/or CD8+ T cells in our CONV lung tissue models are consistent with the reported increase of PD-1$^+$ cells in circulation of CONV [33-36] suggesting that these models are relevant for evaluation of antigen primed responses. Pre-existing T cell Immunity in lungs of UN individuals in our study, however, was represented by M-peptide responder CD8$^+$ stem cell like memory cells, and not N-peptide responding CD8$^+$ T cells as reported by several studies in circulation of UN individuals [6, 7, 14-23]. Interestingly, the change in frequencies of overall N-peptide responding CD8$^+$ T cells were increased signific[33-36]antly in CONV compared to UN. Additionally, the change in N-peptide responding % PD-1$^+$ CD4$^+$T cells

was significantly higher in CONV compared to UN; both not consistent with what is reported in circulation which perhaps reflects the differences in the lung niche that may support local immune responses different from that in circulation.

Previous studies in SARS-CoV recovered individuals have identified persistent memory T cell responses that suggested vaccine-mediated induction of TRMs could be a long-term protection strategy for this pandemic[12]. Consistent with this, a larger proportion of $CD8^+$T cell EM cells and those with TRM phenotype have been identified in bronchoalveolar lavage fluid and lung tissues of individuals with COVID-19[37, 38]. A key role for TRMs in protection against pathogen challenge has been established for many tissues, including the lung[12, 37-39]. Optimal protection against SARS-CoV-infected mice was reported to be conferred by airway TRMs[39]. We report here the existence and long-term maintenance in culture of a high frequency of SARS-CoV-2-S-peptide specific EM $CD8^+$ T cells and TRM in the lungs of CONV individuals. In our studies, 3 out of the 4 CONV showed robust increase in % IFN-γ secreting TRM. While the vaccinated CONV #10 did not demonstrate a significant increase compared to other CONV at baseline, IFN-γ secreting S-peptide responder TRM were increased in this vaccinated CONV. Further, fold change in % TRM of the total IFN-γ^+ cells which were M and N-peptide responders was increased in CONV #10. These observations are consistent with vaccine mediated induction of TRM as a potential long term protection strategy[12, 40]. Additionally, vaccine induced TRM localized to lung tissue of CONV suggest potential beneficial effects in the respiratory tract. Further, the predominant IFN-γ secretion by $CD8^+$ T cells was in response to S-peptide in CONV and the overall TRM response to S-peptide was higher in CONV. In this context, high frequency of spike protein-specific $CD4^+$T cell responses has been reported in blood of COVID-19 CONV [7, 14, 15, 28, 41]. Importantly, $CD4^+$T cells are necessary for the formation of protective $CD8^+$TRM during influenza infection; IFN-γ is an essential signal for this process[42]. Consistent with this, despite the small size in our study, % TRM within $CD4^+$ IFN-γ producers was increased in CONV; a robust 12.5 fold increase in S-

peptide responder TRM was identified within $CD4^+$ cells in CONV #5. Additionally, both IFN-γ secreting $CD4^+$ and $CD8^+$ TRM are responding to both M and N-peptides in addition to S-peptide pools. These data suggest that inclusion of nucleocapsid as well as other structural viral proteins in vaccine approaches may broaden and balance the functional profile of memory T cells, resembling control of natural infection.

Additionally, in this perfusion lung tissue model, we capture B cell responses to SARS-CoV-2 peptide pools against spike protein in CONV lung tissues. The significant change in % S-peptide responding $CD19^+$ cells in CONV compared to UN lung tissues has not been described before. While the B cells in CONV respond to S-peptide pool compared to controls, it remains to be determined with tetramers if the S-peptide responders are antigen-reactive B cells. The increased immature B cell frequencies in the CONV lung tissues may represent what is in circulation, as the lung tissues are not perfused prior to *ex vivo* culture. Nevertheless, this is the first report of a lung tissue model which enumerates local B cell responses in the presence of SARS-CoV-2 antigens in CONV. Organoid models have recently been utilized to assess stimulation with vaccine candidates for SARS-CoV-2[43]; our model which recapitulates lung tissue heterogeneity are comparable to immune organoid cultures to analyze and compare vaccine candidates to new and previously encountered antigens.

METHODS

Clinical Sample Collection: De-identified, remnant surgical specimen were obtained from lobectomy and wedge resection surgeries performed at the University of Alabama at Birmingham. For peptide exposure studies, 12 tissue specimen were obtained from patients with no history of SARS-CoV-2 infection and 4 tissue specimen were obtained from patients who had previously tested positive for SARS-CoV-2 and cleared the infection. This study was approved by the University of Alabama at Birmingham Institutional Review Board (IRB-300003092 and IRB-300003384) and conducted following approved guidelines and regulations. Written informed consent was obtained from all participants. Patient demographics are described in **Table 1**.

Sample Processing and *Ex Vivo* Perfusion Culture: 5 mm diameter tissue cores were generated from remnant surgical specimen using a tissue coring press (Alabama Research and Development, USA). One tissue core was placed into the central chamber of a polydimethylsiloxane (PDMS, Krayden, USA) bioreactor containing a mixture of extracellular matrix (ECM, 90% collagen type 1 (Advanced Biomatrix, USA) + 10% growth factor reduced Matrigel (Corning, USA)) components for structural support as previously described[44]. The tissue/ECM volume was then penetrated with five 400 micron Teflon coated stainless steel wires to generate through-channels for tissue perfusion. Following ECM polymerization, the wires were removed and the through-channels were filled with tissue culture media (1:1 mixture of X-Vivo15 and Bronchial Epithelial Growth media (Lonza, USA) with antibiotics (MP Biomedicals, USA)). The bioreactor was then connected to a perfusion system, that contained a media reservoir, peroxide cured silicon tubing (Cole Parmer, USA), a collection reservoir and peristaltic pump (ESI, USA), and tissue culture media was perfused through the tissue volume for 5 to 14 days (37°C, 5% CO_2), with media changed every 3 days. At the end of each experiment, a portion of each tissue was fixed separately for histologic processing and collagenase B (Roche, Switzerland) digestion for flow cytometry analysis

SARS-CoV-2 Peptide Exposures: For *in vitro* peptide exposures, on day 5 of culture, conditioned media was collected from the collection reservoir and 0.6 nM SARS-CoV-2 peptides (Peptivator peptide pools: M, N and S, Miltenyi Biotec, USA) or vehicle control (cell culture grade water) were added to the tissue chamber of the bioreactor per manufacturer instructions. Following a four hour static incubation, tissue culture media containing brefeldin A and monensin (BD, Germany) was perfused throughout the tissue chamber for an additional 14 hours.

Multiparametric Flow Cytometry: The following antibodies were used for multiparametric flow cytometry for T cell analysis: Anti-CD3-alexafluor 700 (Clone: UCHT1); anti-CD4-FITC (Clone: RPA-T4); anti-CD69-BV563 (Clone: FN50) from BD Biosciences (Germany). Anti-HLA-DR-APC (Clone: LN3); anti-CD3-PE-Cy7 (Clone: UCHT1); anti-CD8-APC (Clone: 53-6.7); anti-Interferon-γ-Alexafluor700 (Clone:B27) from eBioscience (Thermo Fisher, Germany). Anti-Ki-67-Dylight350 (Clone: 1297A) from Novus (USA). Anti-CD45-APC-Cy7 (Clone:2D1); anti-CCR7-Pacific Blue (Clone: G043H7); anti-CD45RA-BV510 (Clone:HI100); anti-CD45RO-PerCy-Cy5.5 (Clone:UCHL1); anti-CD62L-BV650 (Clone:DREG-56); anti-CD103-PE (Clone:Ber-ACT8): anti-CD8-BV510 (Clone:SK1); anti-CD38-PE-Cy7 (Clone:HB-7); anti-CD154-PE/Dazzle (Clone:24-31) anti-PD-1-BV605 (Clone:NAT105); anti-TNF-αBV605 (Clone:MAb11) from Biolegend (USA). The following antibodies were used for multiparametric flow cytometry for analysis of resident immune and structural cells: Anti-CD64-PerCp-eFluor710 (Clone: 10.1); anti-CD11b-APC-Cy7 (Clone: ICRF44); anti-HLA-DR-FITC (Clone: LN3); anti-EpCAM(CD326)-Alexafluor 594 (Clone:9C4) from eBioscience (Thermo Fisher, Germany). Anti-CD16-PE (Clone: 3G8); anti-CD45-Pacific Blue (Clone: HI30); anti-CD66b-PerCP-Cy5.5 (Clone: G10F5) from Biolegend (USA). Anti-CD31-Alexafluor 700 (Clone: UCHT1) from BD Biosciences (Germany) anti-PanCytokerain-APC (Clone: C-11) and anti-Ki-67-Dylight350 (Clone: 1297A) from Novus Biologicals (USA). The following antibodies were used for multiparametric flow cytometry for B cell analysis: anti-CD10-BV650 (Clone:HI10A); anti-CD19-eFluor450 (Clone:HIB19) from eBioscience (Thermo Fisher, Germany). Anti-CD45-BV605 (Clone: 2D1); anti-CD21-PerCP-Cy5

(Clone:Bu32); anti-CD24-APC-Cy7 (Clone:ML5); anti-CD27-APC (Clone: M-T271); anti-CD38-PE-Cy7 (Clone: HB-7); anti-CD138-BV510 (Clone:MI15); anti-IgD-FITC (Clone:IA6-2); anti-IgM-PE (Clone:MHM-88) from Biolegend (USA). The Foxp3 / Transcription Factor Staining Buffer Set (Thermo Fisher, Germany) and the Cytofix/Cytoperm Fixation/Permeablization kit (BD, Germany) were used according to the manufacturer's protocol to stain for intracellular molecules (intranuclear and cytoplasmic molecules, respectively). Analyses were performed on FACSymphony A3 Cell Analyzer with FACSDiva software version 8.0.1 (BD Biosciences, Germany). Data were analyzed with FlowJo 10.7.1 (Treestar, USA).

Histologic Processing and Analysis: Following *ex vivo* culture, a portion of each cultured tissue was fixed with neutral buffered formalin, processed to paraffin, and histological sections were prepared, as previously described[45]. 5 micron sections were stained with hematoxylin and eosin (H&E) to evaluate tissue morphology and cell density (number of cells per cross-sectional area) as described before[46].

Matrix Proteomics: For matrix protein enrichment and extraction, tissue samples were prepared as described before[47]. Briefly, tissues were processed using the Millipore Compartment Protein Extraction Kit with some modifications of the described methodology[47] and all fractions were stored at -80° overnight. The ECM fraction was then reconstituted in 8M urea and deglycosylated. The urea-insoluble fraction was collected by centrifugation, reconstituted in 1x LDS sample buffer, and sonicated for 20 minutes in an ultrasonic water bath. Both urea-soluble and insoluble fractions were quantified via EZQ protein assay, and an equal amount per sample was loaded onto 10% Bis-tris gels and gels were stained overnight with Colloidal Coomassie. Each sample was then digested in 3 fractions with trypsin overnight and high resolution LC-ESI-MS/MS analysis was completed. Data was searched against human subset of Uniref100 database with Carbamidomethylation, Oxidation, and Hydroxyproline.

Measuring Lactate Dehydrogenase: Lactate dehydrogenase (LDH) was measured in conditioned media using the Invitrogen CyQUANT LDH Cytotoxicity Assay (Thermo Fisher, Germany) following manufacturer's instruction.

Statistical Analysis: The measured flow data was summarized by presenting descriptive statistics, such as mean with standard error of the mean (SEM), in the uninfected and convalescent groups. Changes of the measurement between control and each of peptides were computed separately. Two sample t-tests and Wilcoxon rank- sum tests were performed to determine if means of the changes were different between uninfected and convalescent groups. Mean and SD of the outcome measured were estimated by control and peptides within uninfected and convalescent groups respectively. To evaluate difference in the outcome between control and each of peptides within each of the groups, paired t-test and Wilcoxon signed-rank tests were used. All other statistical analyses were performed using SAS 9.4 (SAS Institute, USA). Statistical significance was determined at P-value < 0.05.

ACKNOWLEDGEMENTS

Research reported in this publication was supported by the University of Alabama at Birmingham School of Medicine COVID-19 pilot grant awarded to J.S.D. and was also supported by the UAB Comprehensive Flow Cytometry Core Facility (NIH P30 AR048311 and NIH P30 AI27667), the UAB Tissue Biorepository, and the UAB Pathology Core Research Laboratories. The authors would like to thank Dr. Paul Geopfert for providing insights in T cell immunology in infection.

AUTHOR CONTRIBUTIONS

K.F.G. was involved in bioreactor model set up, experimental design and execution, data collection, data analysis, and manuscript and figure preparation. C.S.S., S.A.K., and A.M.W. were involved in data collection, data analysis, and manuscript editing. Y.W. was involved in data collection and manuscript editing. J.L.B. was involved in bioreactor design and production and

manuscript editing. J.A.M. was involved in the design and analysis of ECM proteomics and manuscript editing. Y.K. was completed statistical analyses and was involved in manuscript editing. V.J.T. and K.S.H were involved in experimental design and reviewing the overall concepts and thought process of the manuscript. M.A. gave critical insights for the manuscript. J.M.D. facilitated collection of remnant surgical specimen and was involved in manuscript editing. J.S.D. was involved in experimental design and oversight, data interpretation, and manuscript and figure preparation.

Correspondence and requests for materials should be addressed to Jessy Deshane (jessydeshane@uabmc.edu)

REFERENCES

1. https://www.biospace.com/article/releases/enzo-announces-issuance-of-u-s-patent-for-methods-of-using-proprietary-compound-sk1-i-in-patients-exploring-options-for-development-as-a-potential-treatment-for-covid-19/.
2. https://www.cdc.gov/coronavirus/2019-ncov/cases-updates/cases-in-us.html. Coronavirus Disease 2019 (COVID-19)-Cases & Latest Updates 2020 3/27/2020 [cited 2020 3/27/2020]; Available from.
3. https://www.worldometers.info/coronavirus/#countries.
4. De Biasi, S. *et al.* Marked T cell activation, senescence, exhaustion and skewing towards TH17 in patients with COVID-19 pneumonia. *Nat Commun* **11**, 3434 (2020).
5. de Candia, P., Prattichizzo, F., Garavelli, S. & Matarese, G. T Cells: Warriors of SARS-CoV-2 Infection. *Trends Immunol* **42**, 18-30 (2021).
6. Files, J.K. *et al.* Sustained cellular immune dysregulation in individuals recovering from SARS-CoV-2 infection. *J Clin Invest* **131** (2021).
7. Le Bert, N. *et al.* SARS-CoV-2-specific T cell immunity in cases of COVID-19 and SARS, and uninfected controls. *Nature* **584**, 457-462 (2020).
8. Toor, S.M., Saleh, R., Sasidharan Nair, V., Taha, R.Z. & Elkord, E. T-cell responses and therapies against SARS-CoV-2 infection. *Immunology* **162**, 30-43 (2021).
9. Farinholt, T. *et al.* Transmission event of SARS-CoV-2 Delta variant reveals multiple vaccine breakthrough infections. *medRxiv* (2021).
10. Olsen, R.J. *et al.* Trajectory of Growth of SARS-CoV-2 Variants in Houston, Texas, January through May 2021 Based on 12,476 Genome Sequences. *Am J Pathol* (2021).
11. Zhao, J. *et al.* Airway Memory CD4(+) T Cells Mediate Protective Immunity against Emerging Respiratory Coronaviruses. *Immunity* **44**, 1379-1391 (2016).
12. Channappanavar, R., Fett, C., Zhao, J., Meyerholz, D.K. & Perlman, S. Virus-specific memory CD8 T cells provide substantial protection from lethal severe acute respiratory syndrome coronavirus infection. *J Virol* **88**, 11034-11044 (2014).
13. Zhao, J., Zhao, J. & Perlman, S. T cell responses are required for protection from clinical disease and for virus clearance in severe acute respiratory syndrome coronavirus-infected mice. *J Virol* **84**, 9318-9325 (2010).
14. Grifoni, A. *et al.* Candidate Targets for Immune Responses to 2019-Novel Coronavirus (nCoV): Sequence Homology- and Bioinformatic-Based Predictions. *SSRN*, 3541361 (2020).
15. Grifoni, A. *et al.* Targets of T Cell Responses to SARS-CoV-2 Coronavirus in Humans with COVID-19 Disease and Unexposed Individuals. *Cell* **181**, 1489-1501 e1415 (2020).
16. Nelde, A. *et al.* SARS-CoV-2-derived peptides define heterologous and COVID-19-induced T cell recognition. *Nat Immunol* **22**, 74-85 (2021).
17. Schulien, I. *et al.* Characterization of pre-existing and induced SARS-CoV-2-specific CD8(+) T cells. *Nat Med* **27**, 78-85 (2021).
18. Kared, H. *et al.* CD8+ T cell responses in convalescent COVID-19 individuals target epitopes from the entire SARS-CoV-2 proteome and show kinetics of early differentiation. *bioRxiv* (2020).
19. Meckiff, B.J. *et al.* Imbalance of Regulatory and Cytotoxic SARS-CoV-2-Reactive CD4(+) T Cells in COVID-19. *Cell* **183**, 1340-1353 e1316 (2020).
20. Ong, E.Z. *et al.* A Dynamic Immune Response Shapes COVID-19 Progression. *Cell Host Microbe* **27**, 879-882 e872 (2020).
21. Parveen, F. *et al.* Role of Ceramidases in Sphingolipid Metabolism and Human Diseases. *Cells* **8** (2019).

22. Rydyznski Moderbacher, C. *et al.* Antigen-Specific Adaptive Immunity to SARS-CoV-2 in Acute COVID-19 and Associations with Age and Disease Severity. *Cell* **183**, 996-1012 e1019 (2020).
23. Sattler, A. *et al.* SARS-CoV-2-specific T cell responses and correlations with COVID-19 patient predisposition. *J Clin Invest* **130**, 6477-6489 (2020).
24. Peng, Y. *et al.* Broad and strong memory CD4(+) and CD8(+) T cells induced by SARS-CoV-2 in UK convalescent individuals following COVID-19. *Nat Immunol* **21**, 1336-1345 (2020).
25. Rodda, L.B. *et al.* Functional SARS-CoV-2-Specific Immune Memory Persists after Mild COVID-19. *Cell* **184**, 169-183 e117 (2021).
26. Jung, J.H. *et al.* SARS-CoV-2-specific T cell memory is sustained in COVID-19 convalescent patients for 10 months with successful development of stem cell-like memory T cells. *Nat Commun* **12**, 4043 (2021).
27. Lipsitch, M., Grad, Y.H., Sette, A. & Crotty, S. Cross-reactive memory T cells and herd immunity to SARS-CoV-2. *Nat Rev Immunol* **20**, 709-713 (2020).
28. Ni, L. *et al.* Detection of SARS-CoV-2-Specific Humoral and Cellular Immunity in COVID-19 Convalescent Individuals. *Immunity* **52**, 971-977 e973 (2020).
29. Tavukcuoglu, E., Horzum, U., Cagkan Inkaya, A., Unal, S. & Esendagli, G. Functional responsiveness of memory T cells from COVID-19 patients. *Cell Immunol* **365**, 104363 (2021).
30. Shaan Lakshmanappa, Y. *et al.* SARS-CoV-2 induces robust germinal center CD4 T follicular helper cell responses in rhesus macaques. *Nat Commun* **12**, 541 (2021).
31. Grigoryan, L. & Pulendran, B. The immunology of SARS-CoV-2 infections and vaccines. *Semin Immunol* **50**, 101422 (2020).
32. Sette, A. & Crotty, S. Pre-existing immunity to SARS-CoV-2: the knowns and unknowns. *Nat Rev Immunol* **20**, 457-458 (2020).
33. Kusnadi, A. *et al.* Severely ill COVID-19 patients display impaired exhaustion features in SARS-CoV-2-reactive CD8(+) T cells. *Sci Immunol* **6** (2021).
34. Boppana, S. *et al.* SARS-CoV-2-specific circulating T follicular helper cells correlate with neutralizing antibodies and increase during early convalescence. *PLoS Pathog* **17**, e1009761 (2021).
35. Gong, F. *et al.* Peripheral CD4+ T cell subsets and antibody response in COVID-19 convalescent individuals. *J Clin Invest* **130**, 6588-6599 (2020).
36. Rha, M.S. *et al.* PD-1-Expressing SARS-CoV-2-Specific CD8(+) T Cells Are Not Exhausted, but Functional in Patients with COVID-19. *Immunity* **54**, 44-52 e43 (2021).
37. Liao, M. *et al.* Single-cell landscape of bronchoalveolar immune cells in patients with COVID-19. *Nat Med* **26**, 842-844 (2020).
38. Grau-Exposito, J. *et al.* Peripheral and lung resident memory T cell responses against SARS-CoV-2. *Nat Commun* **12**, 3010 (2021).
39. Wu, T. *et al.* Lung-resident memory CD8 T cells (TRM) are indispensable for optimal cross-protection against pulmonary virus infection. *J Leukoc Biol* **95**, 215-224 (2014).
40. Channappanavar, R., Zhao, J. & Perlman, S. T cell-mediated immune response to respiratory coronaviruses. *Immunol Res* **59**, 118-128 (2014).
41. Sekine, T. *et al.* Robust T Cell Immunity in Convalescent Individuals with Asymptomatic or Mild COVID-19. *Cell* **183**, 158-168 e114 (2020).
42. Oja, A.E. *et al.* Trigger-happy resident memory CD4(+) T cells inhabit the human lungs. *Mucosal Immunol* **11**, 654-667 (2018).
43. Wagar, L.E. *et al.* Modeling human adaptive immune responses with tonsil organoids. *Nat Med* **27**, 125-135 (2021).
44. Goliwas, K.F. *et al.* Methods to Evaluate Cell Growth, Viability, and Response to Treatment in a Tissue Engineered Breast Cancer Model. *Sci Rep* **7**, 14167 (2017).

45. Goliwas, K.F., Miller, L.M., Marshall, L.E., Berry, J.L. & Frost, A.R. Preparation and Analysis of In Vitro Three Dimensional Breast Carcinoma Surrogates. *J Vis Exp* (2016).
46. Goliwas, K.F. *et al.* Extracellular Vesicle Mediated Tumor-Stromal Crosstalk Within an Engineered Lung Cancer Model. *Front Oncol* **11**, 654922 (2021).
47. Naba, A., Clauser, K.R. & Hynes, R.O. Enrichment of Extracellular Matrix Proteins from Tissues and Digestion into Peptides for Mass Spectrometry Analysis. *J Vis Exp*, e53057 (2015).

FIGURE LEGENDS

Figure 1*: Ex Vivo* Perfusion Culture of Human Lung and Exposure to SARS-CoV-2 Peptides. **A**. *Ex vivo* model setup process. **B**. Bioreactor chamber showing ECM volume containing tissue. **C**. Peptide exposure protocol.

Figure 2: Local T Cell Response to SARS-CoV-2 Peptides within Lung Tissue Cores. **A-G.** Baseline T cell differences within uninfected (UN) and convalescent (CONV) lung tissue. **H-N.** Impact of SARS-CoV-2 peptide exposure on T cell populations in UN and CONV lung tissue. n=8 UN and n=4 CONV. Statistics shown in blue are comparisons between control and peptide exposed samples within each group (UN and CONV). Statistics shown in black are the change in response between UN and CONV for each peptide when compared to the corresponding control.

Figure 3: Memory T Cell Response to SARS-CoV-2 Peptides within the Lung. **A-J.** Baseline differences in memory T cells within uninfected (UN) and convalescent (CONV) lung tissue. **K-T.** Impact of SARS-CoV-2 peptide exposure on memory T cell populations in UN and CONV lung tissue. n=8 UN and n=4 CONV. Statistics shown in blue are comparisons between control and peptide exposed samples within each group (UN and CONV). Statistics shown in black are the change in response between UN and CONV for each peptide when compared to the corresponding control.

Figure 4: Local B Cell Response to SARS-CoV-2 Peptides within the Lung. **A-G.** Baseline differences in B cell populations within uninfected (UN) and convalescent (CONV) lung tissue. **H-N.** Impact of SARS-CoV-2 peptide exposure on B cell populations in UN and CONV lung tissue. n=4 UN and n=3 CONV. Statistics shown in blue are comparisons between control and peptide exposed samples within each group (UN and CONV). Statistics shown in black are the change in response between UN and CONV for each peptide when compared to the corresponding controls.

Figure 1

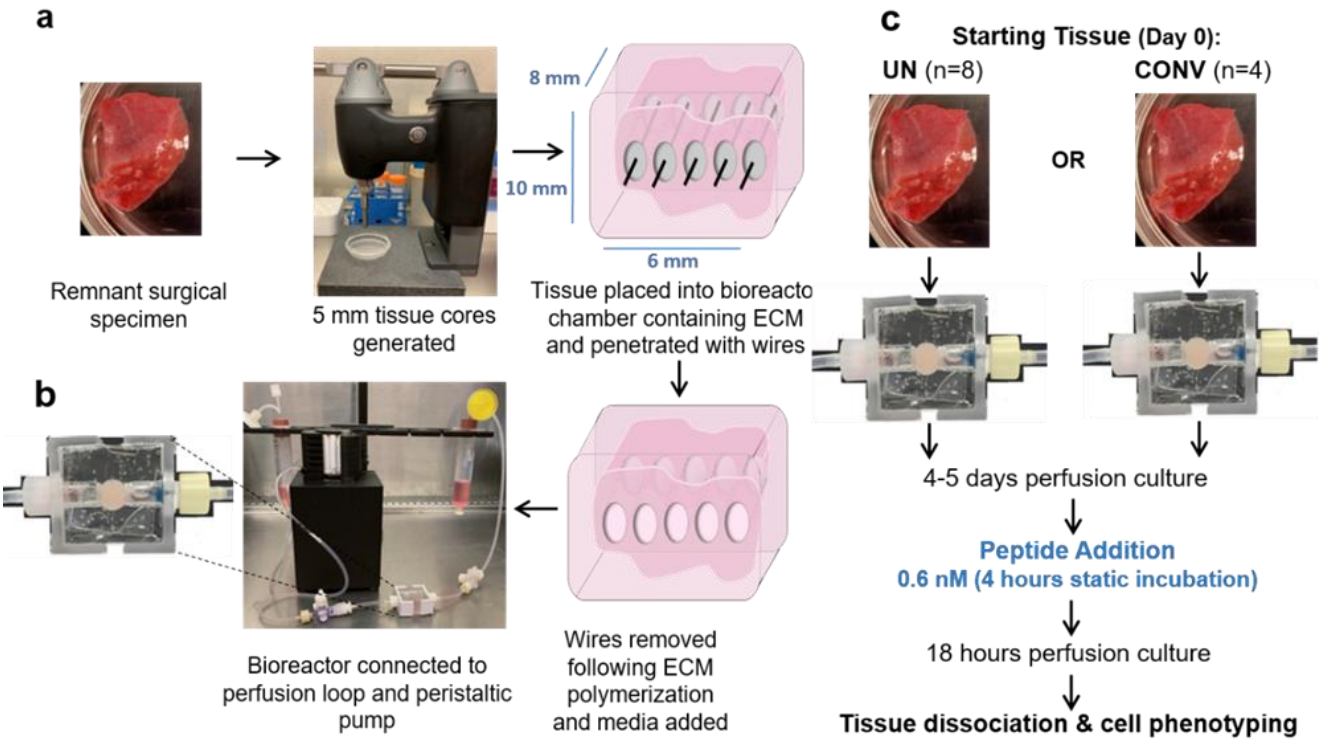

Figure 2

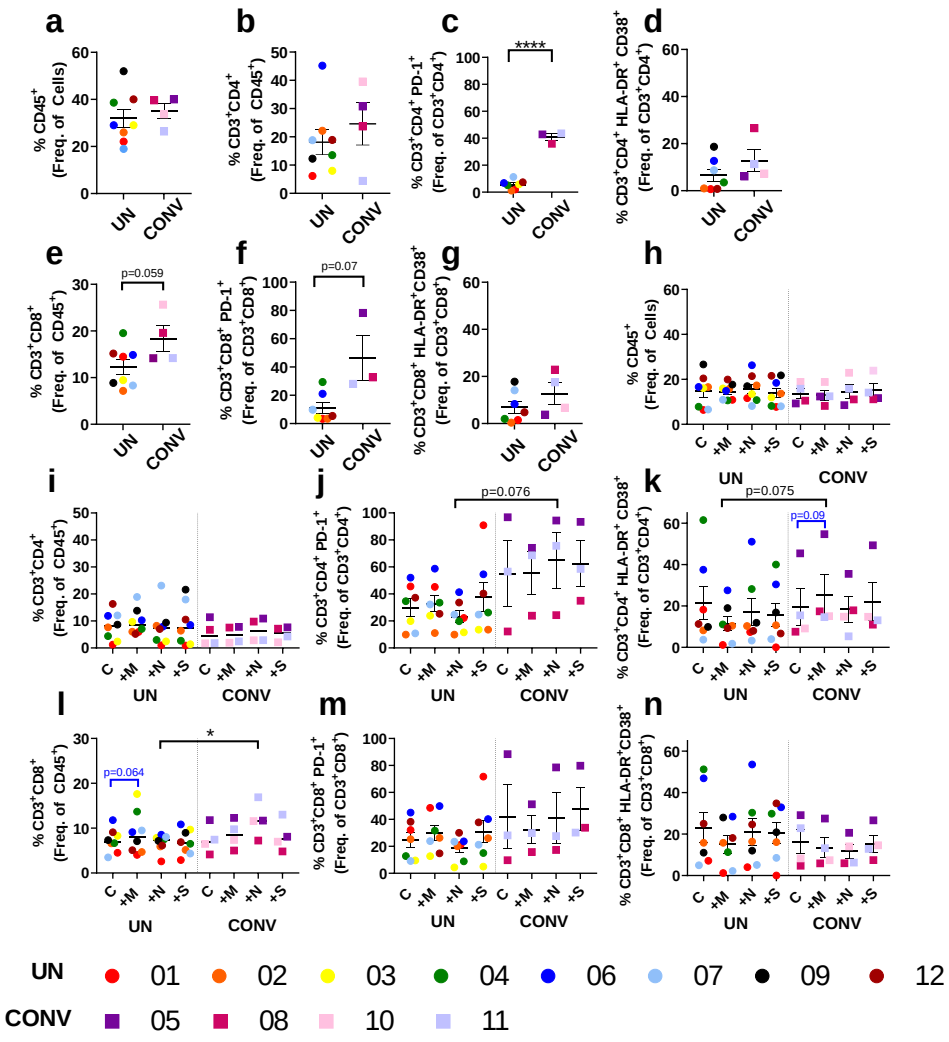

Figure 3

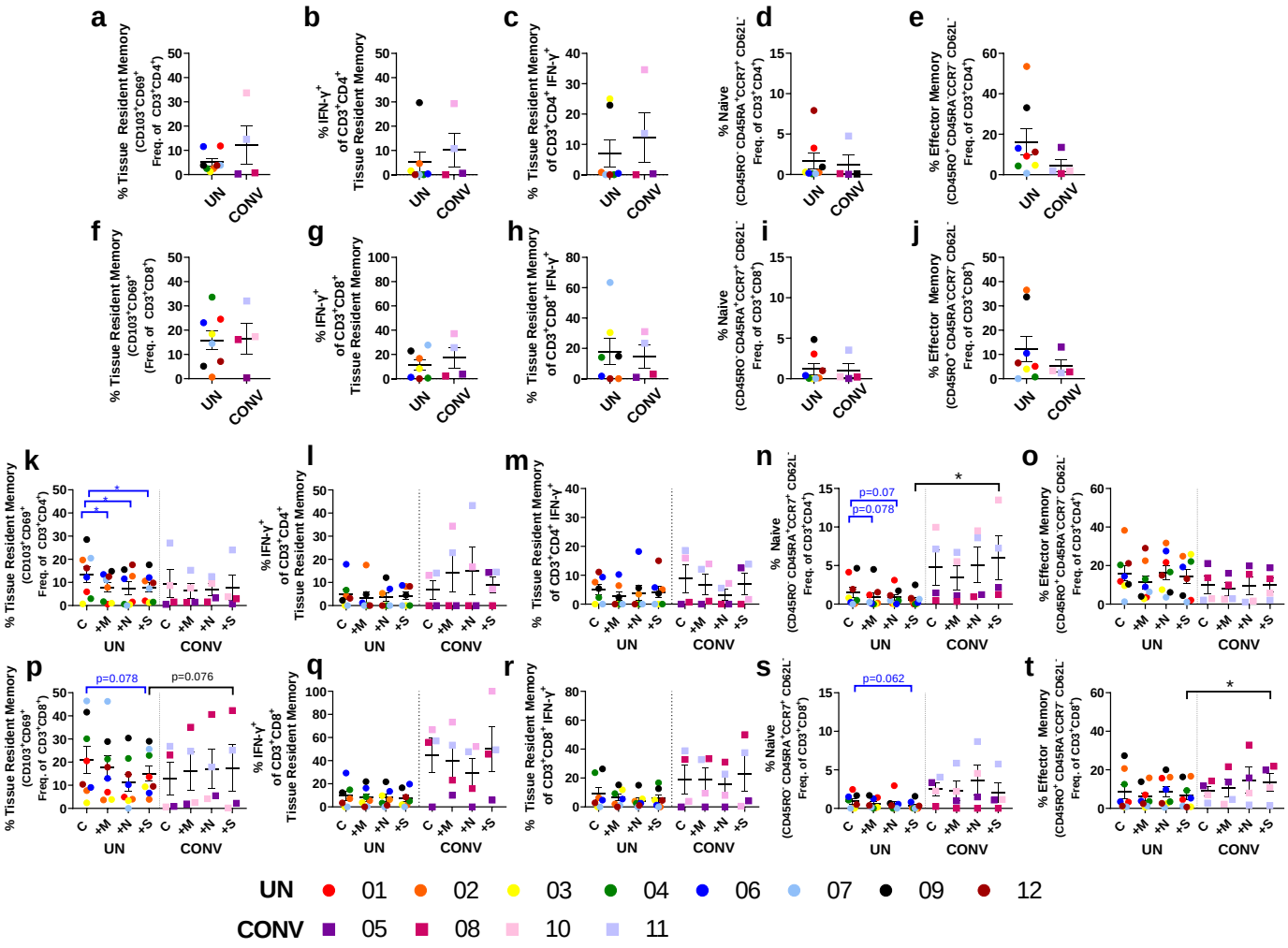

Figure 4